BUCKLING OF CONCRETE SHELLS: A SIMPLIFIED NUMERICAL APPROACH

MATTHIAS ANDRES [a] and REINHARD HARTE [b]

[a] Dr.-Ing. Wayss & Freytag Ingenieurbau AG, Frankfurt am Main,
[b] Prof. at Bergische Universität, Pauluskirchstrasse 7, 42285 Wuppertal, Germany

Editor's Note: Manuscript submitted 28 October 2005; revision received 14 June 2006; accepted for publication 4 September 2006. This paper is open for written discussion, which should be submitted to the IASS Secretariat no later than August 2007.

SUMMARY

In 2004, the paper of Stefan Medwadowski on "Buckling of Concrete Shells: An Overview" [16] presented an excellent overlook over the state-of-the-art of classical stability methods and its application to concrete shells. The respective algorithms in finite-element-method have only been touched, but not discussed in detail. The present paper will give a review of former and new developments in the numerical simulation procedures of buckling phenomena. On one hand, the progress in the development of numerical tools to simulate nonlinearity in concrete structures is significant. On the other hand, there is still a vital need for engineering experience and imagination in order to interpret and value the results correctly. Thus the present paper will consecutively fit to the Medwadowski paper [16]. Besides a more realistic consideration of material nonlinearity in reinforced concrete composite as well a more practical numerical approach will be given.

Keywords: *Buckling, Stability, High-Performance Concrete, Shell Structure, Nonlinear, Material Law, Damage, Cooling Tower*

1. INTRODUCTION

The paper [16] was concentrated on the analytical procedure to describe the buckling mechanism of concrete shell structures. The progress in describing and evaluating of buckling loads of concrete shells started already in the Seventies. The analytical methods have the advantage to use few diagrams and more or less simple formulas to analyse the global (acc. Kollar) or local (acc. Mungan) buckling load of a shell. The main disadvantage is the limited applicability. This only allows the prediction for some theoretical cases, but is not appropriate for complex shell structures with non-symmetric boundary conditions and/or loadings.

The present paper describes an approach to find more realistic buckling loads for various shell structures. This approach is developed as an alternative to a time-consuming, fully nonlinear analysis. It will show a procedure to evaluate realistic buckling loads and corresponding mode patterns with less effort, but still considering the nonlinear concrete behaviour by assuming adequate concrete damage. This might be helpful for the designing engineer to test the structure against buckling failure during the design phase and to evaluate the optimal shape of the shell.

2. FINITE ELEMENT FORMULATION

For the discretization of a shell structure within the scope of a finite element model, an isoparametric four-noded finite element (ASE4-element) [18] formulated in Reissner-Mindlin theory has been taken. The shell element is formulated as an assumed-strain element to avoid locking effects [22]. For the realistic description of the nonlinear material behavior of the material concrete it is necessary to get information about the stress and strain distribution over the height of a cross-section. Thus the layered shell element approach, as it was used in [24] for a different element approach, has been adopted in the following. The different layers can describe both the concrete and the reinforcement steel layers so that the stiffness of the cross-section is considered realistically. To receive the overall stiffness matrix of the structure, which is the central purpose of each finite element analysis, the multi-level strategy [11] (figure 1) is used. This allows the description of the material behaviour on the level of the material point and the improvement of the model for various material properties.

An extremely important issue in buckling analysis is the precise simulation of geometric imperfections of a shell structure. In general, these imperfections lead to a drastic reduction of the overall buckling load so that they have to be considered close to reality. For this purpose an artificial displacement vector is added to the perfect geometry, and considering this vector all relevant geometric properties will change and have to be defined new. At the beginning of an analysis it is not easy to identify the most conservative pattern of this additional imperfection vector with respect to lowest buckling loads. In general an imperfection pattern affine to the lowest eigenmode has been used [9], but some actual publications have been shown that this assumption might not necessarily be the worst imperfection pattern in any case [7]. Nevertheless this approach has proved to be a good starting point so that it was applied for the following investigations, too.

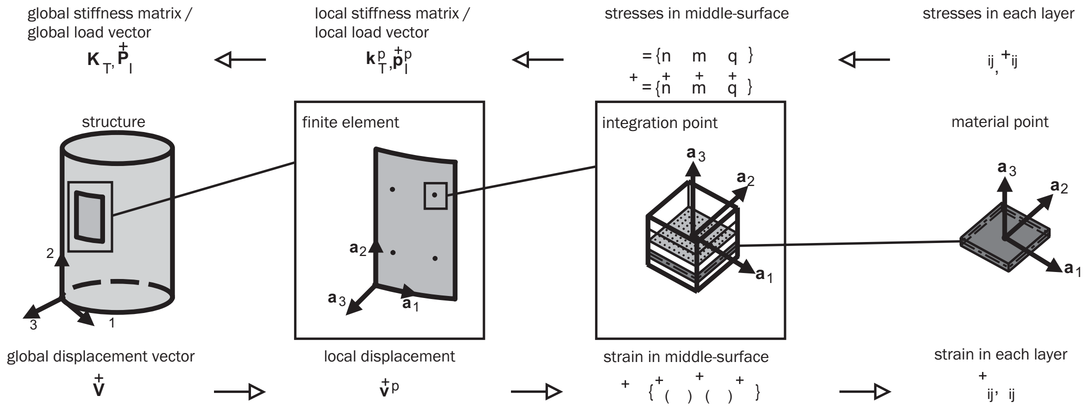

Figure 1. *Multi-level structural analysis concept*

3. ELASTO-PLASTIC MATERIAL MODEL FOR HIGH STRENGTH CONCRETE UNDER CONSIDERATION OF DAMAGE

The recent progress in the development of high strength concrete was one of the main motivations for the presented research work. To describe the material properties of this kind of concrete many experiments have been performed in various research centres in the near past. These experiments serve as a source of each material description and lead to the specific regulations in international and national code. In Germany the new code DIN 1045-1 for concrete structures has been installed in 2001 [8]. In this code the use of nonlinear analysis methods has been regulated for the first time in Germany.

For numerical modelling of the nonlinear material properties within a finite-element-system, the approach of [6] has been chosen in order to get a most flexible formulation for the material law. This approach transforms the mainly biaxial stress state of a concrete shell structure into two separate directions, which can be described with uniaxial material models, which in general are the only information given in code regulations. Thus the model assumes an incremental linear orthotropic stress state in the concrete. With the equivalent Poisson's ratio of $\nu = \sqrt{\nu_1 \cdot \nu_2}$ the material law results in Equation (1).

This biaxial stress state then can be expressed by two equivalent stress-strain relations in principal stress directions. After a transformation the strains results in Equation (2).

Under consideration of the biaxial fracture criterion of [4] the stress-strain relations can be formulated. The ascending branch of this uniaxial relation can be described by the use of [8]

$$\begin{bmatrix} d\sigma_1 \\ d\sigma_2 \\ d\tau_{12} \end{bmatrix} = \frac{1}{1-\nu^2} \begin{bmatrix} E_1 & \nu\sqrt{E_1 E_2} & 0 \\ \nu\sqrt{E_1 E_2} & E_2 & 0 \\ 0 & 0 & \frac{1}{4}\left(E_1 + E_2 - 2\nu\sqrt{E_1 E_2}\right) \end{bmatrix} \cdot \begin{bmatrix} d\varepsilon_1 \\ d\varepsilon_2 \\ d\gamma_{12} \end{bmatrix}. \quad (1)$$

$$\begin{bmatrix} d\varepsilon_{1u} \\ d\varepsilon_{2u} \end{bmatrix} = \frac{1}{1-\nu^2} \begin{bmatrix} 1 & \nu\sqrt{E_2/E_1} \\ \nu\sqrt{E_1/E_2} & 1 \end{bmatrix} \cdot \begin{bmatrix} d\varepsilon_1 \\ d\varepsilon_2 \end{bmatrix} \quad (2)$$

$$\sigma_i = \frac{k\eta - \eta^2}{1 + (k-2)\eta} \cdot f_{cR} \quad (3)$$

with $\eta = \varepsilon_{ic}/\varepsilon_{c1}$ and $k = -1.1 \cdot E_{cm} \cdot \varepsilon_{c1}/f_c$.

(with: ε_{ic} - actual equivalent strain in direction i, ε_{c1} - strain at maximum compressive stress, E_{cm} - mean value of Young`s modulus, ε_{c1}/f_c - calculated mean value of compressive strength for nonlinear analysis).

With respect to [8] the descending branch can be modelled with a linear and a nonlinear part within the finite-element-analysis. This makes it possible to modify the slope according to the fracture energy G_c and the equivalent length of the finite element $l_{eq} = \sqrt{A^e/n_{\text{int}}}$ (with A^e - area of the finite element, n_{int} - number of integration points) in every material point [20].

The composite material reinforced concrete has the well-known ability to carry higher loads than the pure reinforcement layers in the cracked state. The residual load-carrying capacity of the concrete between cracks is dependent on the bond characteristics between steel and concrete matrix. To model this so-called tension-stiffening effect, the concept of iterative simulation according to [19] has been used in this analysis.

4. NONLINEAR ELASTIC AND INELASTIC STABILITY ANALYSIS

4.1 General

In case of conservative static loading the common equation of motion can be reduced to the tangential form:

$$\mathbf{K}_T \cdot \overset{+}{\mathbf{V}} = \mathbf{P}_a - \mathbf{F}_i. \quad (4)$$

This equation is the base of any nonlinear finite-element-analysis. Here $\mathbf{K}_T$ denotes the tangential stiffness matrix, $\mathbf{P}_a$ the given load vector, $\mathbf{F}_i$ the inner force vector of the structure. The tangential stiffness matrix can be decomposed into three parts, the elastic stiffness matrix $\mathbf{K}_e$, the initial stress matrix $\mathbf{K}_\sigma$ and the initial displacement matrix $\mathbf{K}_u$. Further decomposition with respect to linear (L) and nonlinear (NL) dependency on the displacements leads to

$$\begin{aligned} \mathbf{K}_T &= \mathbf{K}_e + \mathbf{K}_\sigma + \mathbf{K}_u \\ &= \mathbf{K}_e + \mathbf{K}_\sigma^L + \mathbf{K}_u^L + \mathbf{K}_\sigma^{NL} + \mathbf{K}_u^{NL}. \end{aligned} \quad (5)$$

The numerical treatment of nonlinear finite-element-simulations and the tracing of the nonlinear structural response branches have been intensively investigated in the past [13, 21].

4.2 The definition of stability and criteria to describe the loss of stability

In science the expression 'stability' has various definitions depending on the respective faculty of science. In structural mechanics ‘stability’ describes the stable equilibrium state of a structure. This leads automatically to the definition of ‘loss of stability’, which means the change from a stable into an unstable state of equilibrium during the load history. The neutral point between stable and unstable equilibrium states of a structure can be characterized by its possible deformations. For stable equilibrium states a distinct displacement pattern exists, and additional displacements directly correspond to rising loads on the structure. The behaviour of the structure at the limit point of stable equilibrium is completely different. Here the response of the structure due to the loading is not unique and at least various response paths are possible.

Loss of stability at the limit point is characterized by two phenomena, snap-through behaviour or bifurcation. In both cases the nonlinear load-displacement branch before buckling is described as the prebuckling state, the branch after buckling as the postbuckling state. To find such multiple equilibrium states within a nonlinear analysis, different algorithms and criteria can be formulated and checked. Equations (4,5) lead to the formulation of

$$\mathbf{K}_T \cdot \overset{+}{\mathbf{V}}_{alt} = \mathbf{0} \qquad (6)$$

in the neutral equilibrium point. This formulation means that an increase of displacements is possible without further load increase. Equation (6) is fulfilled, if the determinant of the tangential stiffness matrix is zero. To evaluate the determinant of the stiffness matrix, the single values in the stiffness matrix in general have to be scaled in order not to exceed the range of computer-precision by multiplications. The expressiveness of the parameter is not high for the observation of reinforced concrete shell structures, because its decrease down to the point of neutral equilibrium is low. Anyway, the occurrence of the neutral state can be definitely identified by this parameter.

Another observation parameter is the so-called stiffness parameter according to Bergan [2]. This parameter, described in equation (7), combines the actual stiffness state with the actual displacement state:

$$S_P = \left(\frac{\Delta\lambda_i}{\Delta\lambda_1}\right)^2 \cdot \frac{\overset{+}{\mathbf{V}}{}_1^T \cdot \mathbf{K}_{T1} \cdot \overset{+}{\mathbf{V}}_1}{\overset{+}{\mathbf{V}}{}_i^T \cdot \mathbf{K}_{Ti} \cdot \overset{+}{\mathbf{V}}_i}\,. \qquad (7)$$

(with: $\Delta\lambda_i$ - incremental load step, $\mathbf{K}_{Ti}$ - tangential stiffness matrix, $\overset{+}{\mathbf{V}}_i$ - incremental displacement vector, i – denotes step i).

In case of snap-through behaviour, the parameter will be zero, whereas in case of bifurcation behaviour in the neutral equilibrium state the parameter will not be able to definitely identify the loss stability.

Another possible criterion is the observation of the diagonal values D_{ii} of the tangential stiffness matrix. In the state of stable equilibrium all diagonal values are positive, whereas in the unstable state at least one value is getting negative. This is the reason why the authors of this paper have performed complete nonlinear analyses accompanied by the observation of all parameters listed in table 1.

State of equilibrium	Stiffness-parameter	determinant $\mathbf{K}_T$	Diagonal values
stable	$S_P \neq 0$	$\det \mathbf{K}_{Td} > 0$	$\forall\, D_{ii} > 0$
neutral (snap-through point)	$S_P = 0$	$\det \mathbf{K}_{Td} = 0$	$\exists\, D_{ii} = 0$
neutral (bifurcation point)	$S_P \neq 0$	$\det \mathbf{K}_{Td} = 0$	$\exists\, D_{ii} = 0$
unstable	$S_P \neq 0$	$\det \mathbf{K}_{Td} \neq 0$	$\exists\, D_{ii} < 0$

Table 1. *Parameters for identification of critical states of equilibrium*

4.3 Accompanying eigenvalue analysis

In addition to the observation of the above given different parameters during the nonlinear analysis algorithm the following eigenvalue problem can be solved in each load step of the analysis:

$$\left\{\mathbf{K}_e + \Lambda \cdot \left(\mathbf{K}^L + \mathbf{K}^{NL}\right)\right\} \cdot \mathbf{\Psi} = \mathbf{0} \qquad (8)$$

The expected limit load level, in which stability failure occurs, can be found by multiplying the actual load factor with the calculated eigenvalue. This well-known algorithm delivers good estimations for elastic structures, but considering material nonlinearity the results in general will have poor quality. Anyway, points of neutral equilibrium can be definitely identified by this method, if sufficient numerical preciseness is given in order not to miss the lowest bifurcation point on the load path.

4.4 Structural damage and its consideration within a stability analysis

To describe the influence of structural damage on the stability behaviour, different states of deformation have to be defined in order to evaluate the incremental form of equation (5) in a similar way as considering geometrical imperfections. This is shown in detail in figure (2).

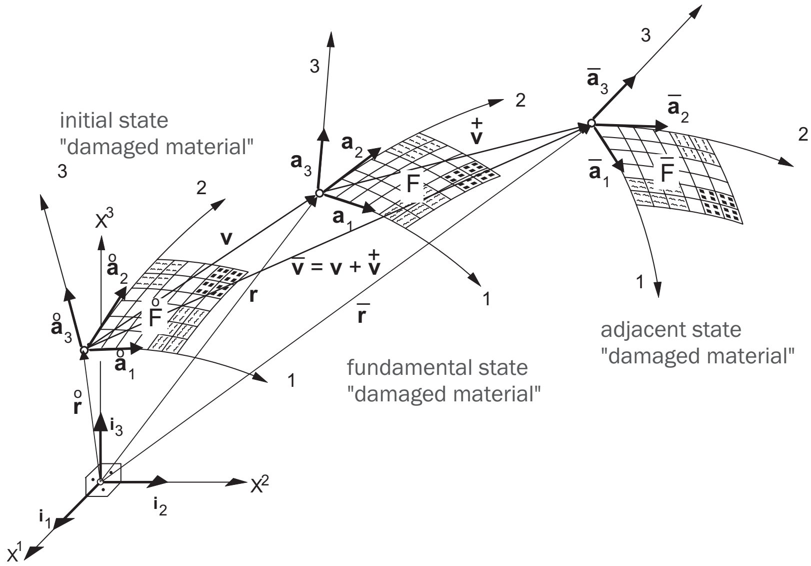

Figure 2. *Incremental approach under consideration of initial damage*

The decomposition of the tangential stiffness matrix looks like

$$\begin{aligned}\mathbf{K}_{Td} &= \mathbf{K}_{ed} + \mathbf{K}_{\sigma d}^{L} + \mathbf{K}_{ud}^{L} + \mathbf{K}_{\sigma d}^{NL} + \mathbf{K}_{ud}^{NL} \\ &= \mathbf{K}_{ed} + \qquad \mathbf{K}_{d}^{L} \qquad + \qquad \mathbf{K}_{d}^{NL}\end{aligned} \tag{9}$$

where index (d) symbolises the damage of the structure.

The eigenvalue problem given in equation (8) can be formulated in a modified form:

$$\left\{\mathbf{K}_{ed} + \Lambda \cdot \left(\mathbf{K}_{d}^{L} + \mathbf{K}_{d}^{NL}\right)\right\} \cdot \mathbf{\Psi} = \mathbf{0}\,. \tag{10}$$

To simulate the material properties in different directions and to evaluate the modified stiffness matrix $\mathbf{K}_{ed}$, the material law is formulated according to anisotropic plate behaviour. Hereby different properties like thickness and/or stiffness can be defined separately in two directions. The properties in both directions are coupled via Poisson's ratio. Then the overall stiffness must be defined with the stiffness of the separate directions.

In case of cracking the axis of inertia will be shifted. The value of the resulting eccentricity can be analysed by

$$e_{ges} = \frac{\left(\frac{h}{2} \pm \frac{t_{crack}}{2}\right) \cdot E_c \cdot \left(h - t_{crack}\right) + E_s \cdot \sum_i a_{si} \cdot e_{si}}{E_c \cdot \left(h - t_{crack}\right) + E_s \cdot \sum_i a_{si}} - \frac{h}{2} \tag{11}$$

where E_s and E_c denote the Young's moduli of reinforcement steel and of concrete; the other quantities can be taken from figure 3.

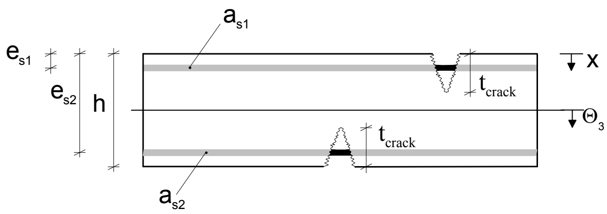

Figure 3. *Shift of axis of inertia for a cracked reinforced concrete cross section*

Considering the well-known coupling terms of anisotropic plate theory for the characterisation of the interaction between tension and bending, the approximate state of stiffness can be determined in each finite element.

The parameters, which are necessary to model the different stiffness characteristics, can be defined separately for damage-inducing strains and for the different material components (figure 4). The damage of concrete due to compression can be simulated according to the stress-strain law, applying the secant Young's modulus E_d, as shown in figure 4. To evaluate the overall damage this parameter has to be integrated over all layers of the cross section:

$$D^{comp} = \frac{\sum_i D_i \cdot h_i}{h} \qquad \text{with} \quad D_i = 1 - \frac{E_d}{E_0}\,. \tag{12}$$

The description of the damage of concrete due to tension is much easier. Only two states of damage may exist. If the layer is cracked the parameter is $D=1$, whereas in the uncracked state it is $D=0$. The overall damage of the cross-section then again can be evaluated by integration over cross-section height:

$$D^{ten} = \frac{h-t_{crack}}{h}. \tag{13}$$

The damage component of the reinforcement steel can be defined with the help of the secant Young's modulus, where $D=1$ denotes the total yielding of the cross-section.

$$D^{steel} = \frac{E_0 - E_d}{E_0 - E_{d,\max}}. \tag{14}$$

These damage parameters make it possible to reduce the stiffness of each finite element separately, with respect to the actual state of loading and the corresponding stresses.

To identify, whether the damage has a reducing effect on the stiffness or not, case differentiations with respect to the different kinds of damage have to be defined. For example table 2 shows the case differentiation for crack damage. As a criterion the strains at the inner ($\gamma_{\alpha\alpha}(-h/2)$) and the outer surface ($\gamma_{\alpha\alpha}(+h/2)$) of an element have been taken. These two values define the strain state, and by linear transformation the stress state of the observed element can be delivered. For example a cross section has been damaged by cracks and should be stressed in tension again. Then both tensile and bending stiffness will be reduced. If the cross-section will be stressed in compression, only the bending stiffness has to be reduced, as the concrete cross-section can bear the compressive load again by closing the cracks. From a theoretical viewpoint this is not exact, because the bending stiffness will as well rise in case of increasing compression, but this stiffness increase is not very stable. In case of only small disturbances the cross-section would loss the bending stiffness automatically, which from a safety point cannot be

	$\gamma_{\alpha\alpha}\left(+\frac{h}{2}\right)<0$	$\gamma_{\alpha\alpha}\left(+\frac{h}{2}\right)=0$	$\gamma_{\alpha\alpha}\left(+\frac{h}{2}\right)>0$
$\gamma_{\alpha\alpha}\left(-\frac{h}{2}\right)<0$	$B_{\alpha\alpha}$	$B_{\alpha\alpha}$	$D_\alpha^{ten}>0 \Rightarrow D_{\alpha\alpha}, B_{\alpha\alpha}$ $D_\alpha^{ten}<0 \Rightarrow B_{\alpha\alpha}$
$\gamma_{\alpha\alpha}\left(-\frac{h}{2}\right)=0$	$B_{\alpha\alpha}$	$B_{\alpha\alpha}$	$D_\alpha^{ten}>0 \Rightarrow D_{\alpha\alpha}, B_{\alpha\alpha}$ $D_\alpha^{ten}<0 \Rightarrow B_{\alpha\alpha}$
$\gamma_{\alpha\alpha}\left(-\frac{h}{2}\right)>0$	$D_\alpha^{ten}<0 \Rightarrow D_{\alpha\alpha}, B_{\alpha\alpha}$ $D_\alpha^{ten}>0 \Rightarrow B_{\alpha\alpha}$	$D_\alpha^{ten}<0 \Rightarrow D_{\alpha\alpha}, B_{\alpha\alpha}$ $D_\alpha^{ten}>0 \Rightarrow B_{\alpha\alpha}$	$D_{\alpha\alpha}, B_{\alpha\alpha}$

Table 2. *Case differentiation for crack-damage* D_α^{ten}

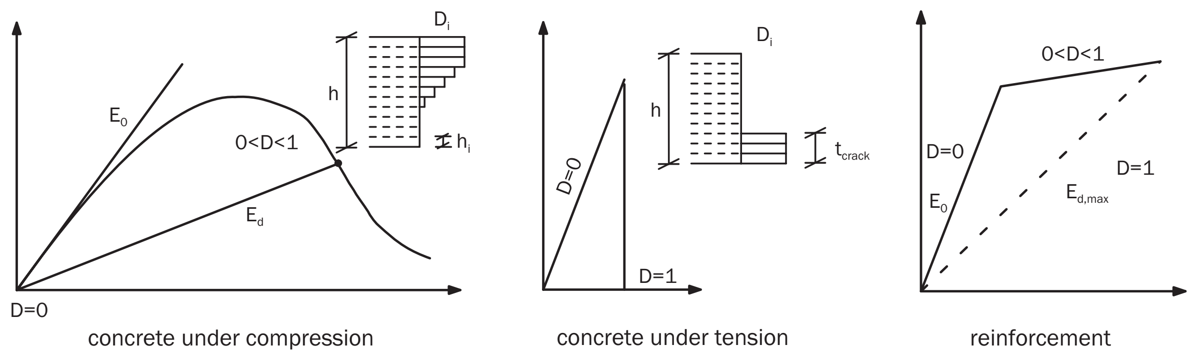

Figure 4. *Definition of local damage parameters*

accepted anyway. Thus the increase of bending stiffness with respect to the state of compression will neglected. More important is to clearly identify the surface of the element on which the crack is initiated.

With these assumptions and with the objective to establish a simple method to calculate buckling loads and modes considering damages, the following iterative approach has been developed:

1. Determination of $\mathbf{K}_{ed,i=1}$ with strain state zero.
2. Solving of $\mathbf{K}_{ed,i=1} \cdot \mathbf{V}_{i=1} = \overset{0}{\mathbf{P}}$.
3. Determination of $\mathbf{K}_{\sigma d,i=1}$.
4. Solving of eigenvalue problem $\left(\mathbf{K}_{ed,i=1} + \Lambda_{i=1} \cdot \mathbf{K}_{\sigma d,i=1}\right) \cdot \mathbf{\Psi} = \mathbf{0}$.
5. Determination of $\mathbf{K}_{ed,i=2}$ under consideration of displacement state $\mathbf{V}_{i=1}$.
6. Solving of eigenvalue problem $\left(\mathbf{K}_{ed,i=2} + \Lambda_{i=2} \cdot \mathbf{K}_{\sigma d,i=1}\right) \cdot \mathbf{\Psi} = \mathbf{0}$.
7. Solving of equilibrium equation $\mathbf{K}_{ed,i=2} \cdot \mathbf{V}_{i=2} = \overset{0}{\mathbf{P}}$.
8. Determination of $\mathbf{K}_{ed,i=3}$ and $\mathbf{K}_{\sigma d,i=2}$ considering the displacement state $\mathbf{V}_{i=2}$.
9. Solving of the eigenvalue problem $\left(\mathbf{K}_{ed,i=3} + \Lambda_{i=3} \cdot \mathbf{K}_{\sigma d,i=2}\right) \cdot \mathbf{\Psi} = \mathbf{0}$.
10. Output of the eigenvalues $\Lambda_{i=1}, \Lambda_{i=2}$ and $\Lambda_{i=3}$.

The quality of the found buckling load factors depends on the quality of the given damage state. With the help of this approach it will become possible to quantify the influence of damages on the buckling behaviour of a shell, while avoiding time-consuming fully nonlinear numerical analyses in some cases. To identify the appropriate damage states and corresponding parameters the authors refer to the results of SFB 398 at the Ruhr University of Bochum [12].

Further damage effects on concrete structures can be initiated by the phenomena of creep and shrinkage, which have a significant influence on the overall behavior of a structure. It will not be considered in the present paper, but has been actually described in the work of [3].

5. BUCKLING ANALYSES OF CONCRETE SHELL STRUCTURES

5.1 Axially compressed cylindrical shell

The axially compressed shell panel is a well-known benchmark test for buckling analysis. The dimensions and boundary conditions of the chosen panel have been adapted from Wolmir [23]. The radius of the panel is taken to $R = 83.33\,\mathrm{m}$, the shell thickness to $t = 0.10\,\mathrm{m}$ and the concrete is chosen as a C100/115 with a reinforcement ratio

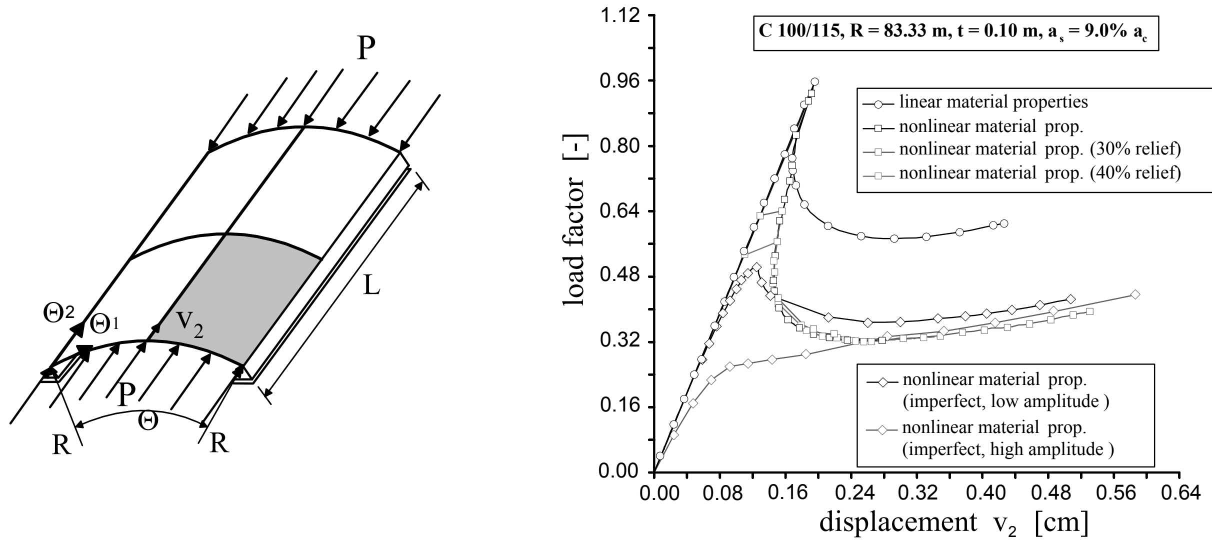

Figure 5. *System and loading of an axial compressed shell panel (left) and load-displacement-curve from a modified stability analysis (right)*

of $\rho = 9.0\%$. The panel can be modelled by an 8x8 finite element mesh, considering symmetric boundary conditions with respect to both axes (Figure 5).

Figure 5 as well gives the load-displacement curves for different levels of nonlinear analysis methods, in comparison with results of a classical geometrically nonlinear analysis with elastic material behaviour. In all cases the load has been increased incrementally close to the point of neutral equilibrium, characterized by snap-through behaviour. After adding a perturbation vector, the response path in the postbuckling range can be found. The magnitude of this perturbation significantly influences the numerical convergence of the solution.

In the geometrically nonlinear, but elastic analysis the well-known response path with the postbuckling minimum on the level of 70% of the linear buckling load is found.

The analysis with the nonlinear material characteristics yields a postbuckling minimum, which drops down to a level of 50% compared with that of the system with linear elastic material. This means that the postbuckling minimum is found at 30% level of the linear buckling load. This minimum, which has to be interpreted as the ultimate limit load of the system, can be detected via different analysis methods. The full analysis of the response path is very time consuming and has a low convergence rate cause of the high numerical instability in the neighbourhood of the point of neutral equilibrium. This effort can be minimized by an analytical decrease of load when approaching this instability point. When decreasing the load, a perturbation vector is added in a similar way as in the full nonlinear analysis. Figure 5 shows also the analysed response paths for different magnitudes of relief and definitely demonstrates that the postbuckling minimum can be detected on the same level. This approach reduces the computation time and leads to a safe identification of the lowest ultimate load.

In addition, the nonlinear analysis was performed considering geometrical imperfections. As can be seen in Figure 5, the response paths are smooth to the response path of the perfect system.

Further investigations have been made considering damage effects, as described in section 4.4. The left part of figure 6 shows the results with different kinds of presumed damage states, characterized by the reduction of the compressive strength in the different Θ^{α} -directions. Best correspondence to the physically nonlinear analysis can be found presuming a damage of 50% in both Θ^1 - and Θ^2 -direction.

Furthermore, the right part of figure 6 shows the results of the modified linear buckling analysis (see section 4.4). Here the damage state at the point of the postbuckling minimum, calculated by the full nonlinear analysis, is taken as an initial state. Even in the first step of analysis a good approximation of the 'real' postbuckling minimum is found. The following iteration step yields a value very close to the postbuckling minimum of the full nonlinear analysis.

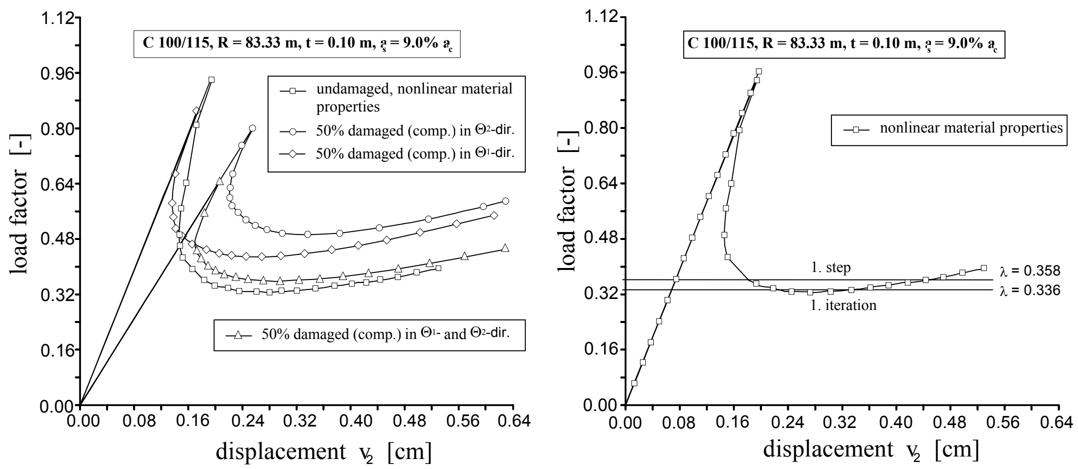

Figure 6. *Load-displacement-curve of an axial compressed shell panel with initial compression damage (left) and results of modified linear stability analysis (right)*

Result: The resulting postbuckling minimum of a geometrical nonlinear analysis, which has often been assumed as the lowest bound, will drop down significantly to 30 % when considering material nonlinearities and initial damages. Thus a safety factor, i.e. $\gamma = 5.0$ in the old German concrete code DIN 1045, ed. 1988, which has been taken in the past for the design of thin concrete shells against buckling, can be confirmed by the previous calculations. With this knowledge a reduction of this factor cannot be justified without further parameter studies.

5.2 Cooling Tower Shell 'Grand Gulf'

Cooling tower shells are typical thin reinforced concrete structures which might be exposed to buckling phenomena. Thus, to apply the presented tools and concepts, the cooling tower of the Grand Gulf Nuclear Power Plant, Mississippi, USA built in 1977 has been taken as example. Unusually, this cooling tower did partly collapse during its erection because of a tornado which hit the central crane. The shell was repaired and the cooling tower was finished, but nevertheless it has been in the focus of many researchers in the past. [14, 15, 17].

Figure 7 shows the discretization with 64x51 ASE4-shell elements of half of the structure due to symmetrical boundary conditions. As well the main dimensions, the distribution of the original thickness and of the inner and outer reinforcement ratio over height are given there.

First, all analyses were made with the material specifications of the originally used materials, taken from [14]. Later the calculations have been repeated taking the specifications of a high strength concrete C80/95. In this case the thickness was reduced by about 4 cm to get comparable results with respect to the critical load level. The reduction of thickness leads to higher stresses due to wind action, which results in higher reinforcement ratios. These ratios have been considered as well. The nonlinear analyses were made for the load combination $\lambda \cdot (G + W)$, with G – dead load, W – wind load and λ - load factor.

The classical linear buckling analysis leads to a buckling factor of $\lambda = 9.3$ for normal concrete and $\lambda = 9.6$ for high-strength concrete. The corresponding buckling modes do not differ significantly.

Figure 8 shows the load-displacement curves of both analyses considering linear and nonlinear material behaviour. The results with linear elastic material specifications show the typical snap-through phenomenon as the relevant mode of failure. The corresponding displacement mode is characterized by a singular buckle in the region of the largest compressive stresses in the lower section of the tower (figure 9).

In case of considering material nonlinearity the structure shows a completely different response. Again the shell's failure is characterized by loss of stability, but now the tower shows a nonlinear load-displacement-relation in the pre-buckling phases because of cracking of concrete in the windward meridian section. Snapping-through occurs at a load level about 30% less that considering linear elastic material behaviour. The corresponding displacement pattern shows a completely different behaviour both in the pre- and in the postbuckling range. The cracking of the shell in the windward meridian section and as well of parts of the upper ring beam lead to buckling in the flanks of the structure sideward to the windward meridian.

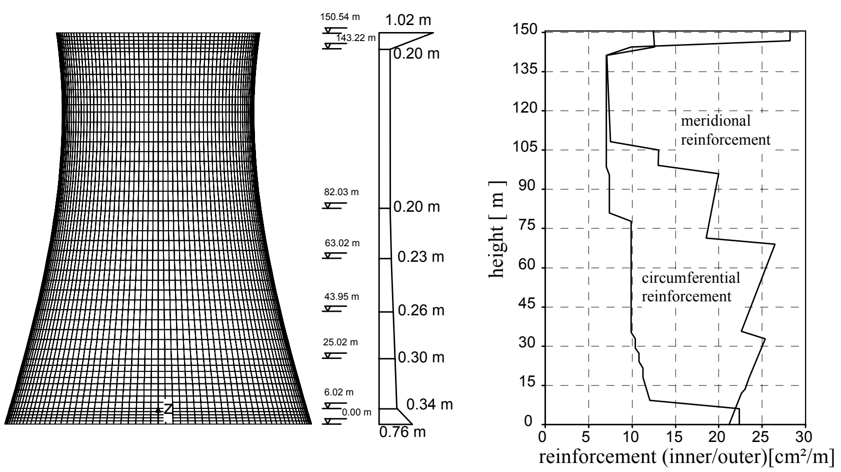

Figure 7. *Discretization, original thickness and given reinforcement ratio (on one side) of the cooling tower Grand Gulf*

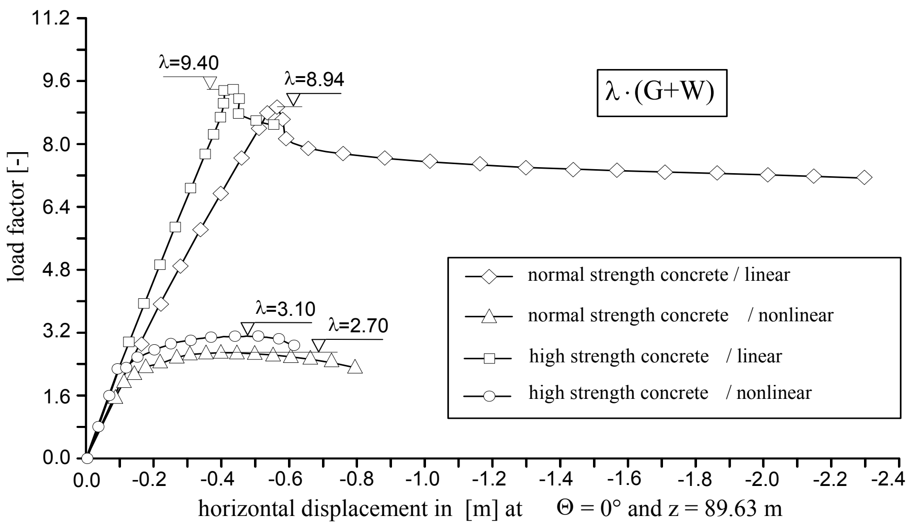

Figure 8. *Load-displacement-curve of different analysis of the cooing tower Grand Gulf*

In case of high strength concrete this behaviour does not differ significantly. But, because of smaller ductility, the post-buckling range is now characterized by considerably less displacements till total failure.

Additionally, the analysis was performed applying the approach presented in section 4.4. Under consideration of the damage state near to the failure state a reduction of about 50% against the classical buckling factor is observed. Within this analysis the damage induced displacements growth is not considered. The detailed results of this example are given in [1].

Result: The presented nonlinear algorithms are suitable for practical application to large scale shell structures. The consideration of material nonlinearity yields buckling loads, which are approx. 70 % lower in comparison to those of a linear elastic analysis. Because of a nearly linear pre-buckling behaviour of a linear elastic analysis the reduction as well is about 70 % lower the classical load via eigenvalue analysis. Thus the retention of a high safety factor, like $\gamma = 5.0$ acc. DIN 1045, ed. 1988, is still justified. It as well includes further reductions of the buckling limit due to imperfections, creep, shrinkage, etc. The derivation of buckling loads via classical eigenvalue analysis will only provide an acceptable approach of the real critical load if the structural behaviour in the pre-buckling state is nearly linear.

6. CONCLUSIONS

It has been demonstrated that the consideration of material nonlinearity may have a significant influence on the stability of reinforced concrete shells. Both in case of bifurcation (axially compressed shell panel) or snap-through (cooling tower), the relevant load limit can be down to 30 % of the results of a linear elastic analysis. This justifies the retention of high safety margins when performing classical stability proofs.

The use of high-strength concrete does not change the phenomenology of the stability behaviour. The advantage of higher strength and greater stiffness can be credited only within certain limits, as the real design of shell structures demands for minimum shell thickness, due to concrete cover in order to avoid corrosion of reinforcement. Thus buckling failure does not seem to be probable, the probability of buckling failure seems to be low. Nevertheless, the combination of high strength concrete with textile, glass or carbon reinforcement [5] might lead to a minimized wall thickness of curved shells. Then the consideration of initial damages will get more importance, and the presented algorithms might allow a realistic approach of the expected stability phenomena.

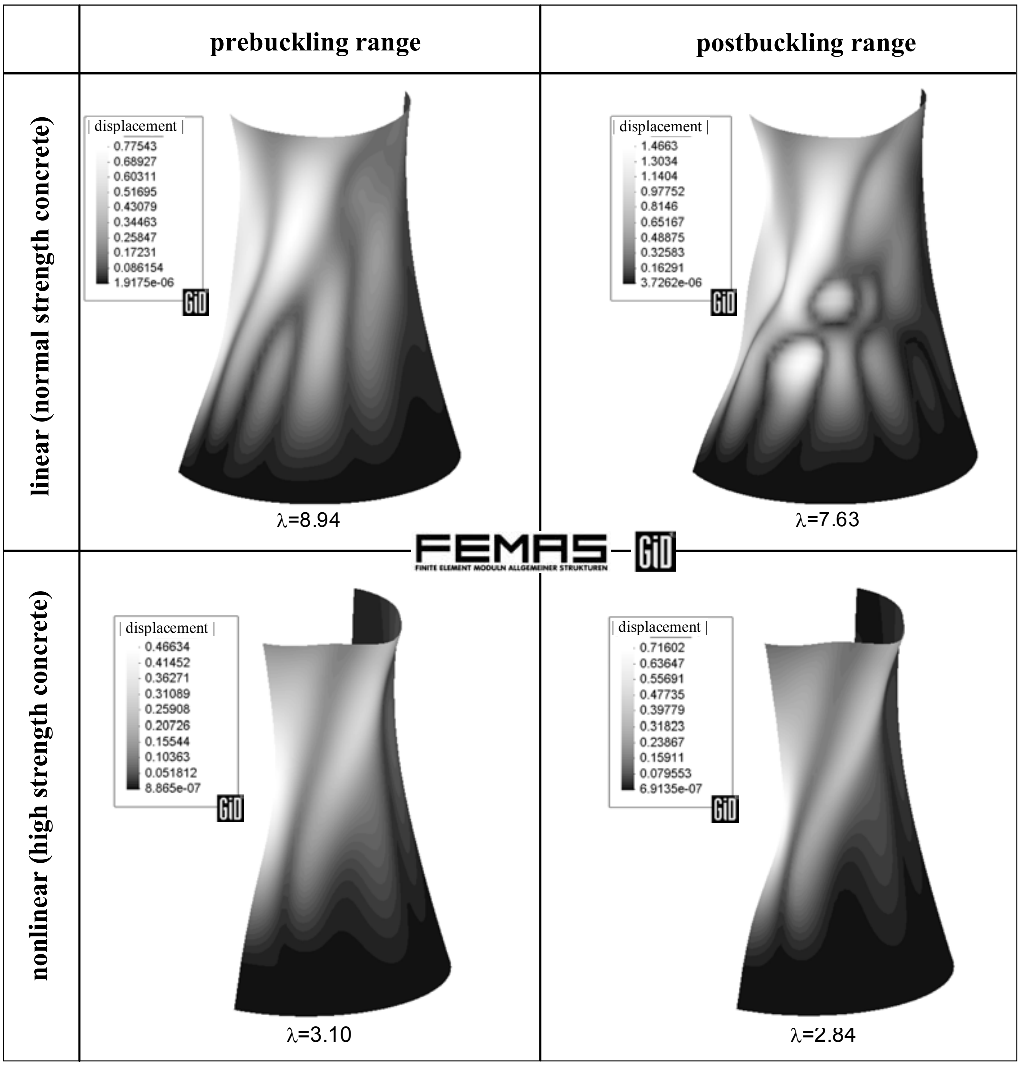

Figure 9. *Displacement patterns in the prebuckling and postbuckling state of a linear and nonlinear analysis*

ACKNOWLEDGEMENTS

The authors want to thank the German Research Foundation DFG for funding most of the research work presented in this paper [1, 10].

REFERENCES

[1] ***Andres, M.*** Zum Stabilitätsnachweis von Schalentragwerken aus Hochleistungsbeton, Dissertation, Bergische Universität Wuppertal, Germany (2004).

[2] ***Bergan, P.G., Horrigmoe, G., Krakeland, B. and Soreide, T.H.*** Solution techniques for nonlinear finite element problems. *Int. J. Numer. Methods Eng.* 12 (1978), 1677-1696.

[3] ***Bockhold, J.*** Modellbildung und numerische Analyse nichtlinearer Kriechprozesse in Stahlbetonkonstruktionen unter Schädigungsaspekten, Schriftenreihe des Instituts für Konstruktiven Ingenieurbau, Heft 2005-6 Ruhr-Universität Bochum, Germany (2005).

[4] ***Curbach, M., Hampel, T., Speck, K. and Scheerer, S.*** Versuchstechnische Ermittlung und mathematische Beschreibung der mehraxialen Festigkeit von Hochleistungsbeton bei zwei- und dreiaxialer Druckfestigkeit, *Zusammenfassung des DFG-Projekts CU 37/1-2*, TU Dresden, Germany (2000).

[5] ***Curbach, M., Wagner, A., Hegger, J. and Will, N.*** Textilbewehrter Beton - Eine innovative Werkstoffkombination, *VDI-Ingenieurtag 2003, Fachkongress „Innovatives Planen und Bauen - Bautechnik für die Gesellschaft von morgen“* VDI-Gesellschaft Bautechnik (2003), 51-70.

[6] ***Darwin, D. and Pecknold, D.A.*** Nonlinear biaxial stress-strain law for concrete, *Journal of the Engineering Mechanics Division* / ASCE 103(EM2) (1977), 229-241.

[7] ***Deml, M.*** Ein Finite-Element-Konzept zur Traglastanalyse imperfektionssensitiver Schalenstrukturen, Berichte aus dem Konstruktiven Ingenieurbau, Nr.6/97, TU München (1997).

[8] ***DIN 1045-1*** *Tragwerke aus Beton, Stahlbeton und Spannbeton – Teil 1: Bemessung und Konstruktion*, Berlin: Beuth Verlag GmbH (2001).

[9] ***Eckstein, U., Harte, R., Krätzig, W.B. and Wittek, U.*** Solution strategies for linear and nonlinear instability phenomena for arbitrarily curved thin shell structures. *Proc. 7th Int. Conf. on Structural Mechanics in Reactor Technology.* Amsterdam: North-Holland (1983), 163-170.

[10] ***Harte, R. and Andres, M.*** Grundsatzuntersuchungen zum Stabilitätsverhalten von Schalenkonstruktionen aus Hochleistungsbeton, *Abschlussbericht des Projekts HA 1031/3 (DFG)*, Bergische Universität Wuppertal, Germany (2004).

[11] ***Krätzig, W.B.*** Multi-level modelling techniques for elasto-plastic structural responses. In: Owen D.R.J., Onate, E., Hinton, E. (eds.): *Computational plasticity*, part 1. Barcelona: Int. Center for Numerical Methods in Engineering (1997), 457-468.

[12] ***Krätzig, W.B., Petryna, Y.S. and Stangenberg, F.*** Measures of structural damage for global failure analysis, *Int. J. of Solids and Structures* 37 (2000), 7393-7407.

[13] ***Krätzig, W.B., Wittek, U. and Basar, Y.*** Buckling of general shells. In: J.M.T. Thompson, G.W. Hunt (Eds.): *Collapse*, Cambridge: Cambridge University Press (1983), 377-394.

[14] ***Mahmoud, B.E.H. and Gupta, A.K.*** Inelastic large displacement behavior and buckling of hyperbolic cooling tower shells, North Carolina State University, USA (1993).

[15] ***Mang, H.A., Floegl, H., Trappel F. and Walter, H.*** Wind-loaded reinforced-concrete cooling towers: Buckling or Ultimate Load, *Engineering Structures* 5 (1983),163-180.

[16] ***Medwadowski, St. J.*** Buckling of concrete shells – an overview, *IASS-Journal* Vol. 45 (2004), n. 1, 51-63.

[17] ***Min, C.S.*** A study of inelastic behavior of reinforced concrete shells using supercomputers, PHD-Thesis, North Carolina State University, USA (1992).

[18] ***Montag, U.*** Konzepte zur Effizienzsteigerung numerischer Simulationsalgorithmen für elastoplastische Deformationsprozesse, Techn.-Wiss. Mitteilung Nr. 97-6, Ruhr-Universität Bochum, Germany (1997).

[19] ***Noh, S.-Y.*** Beitrag zur numerischen Analyse der Schädigungsmechanismen von Naturzugkühltürmen, Dissertation, RWTH Aachen, Germany (2001).

[20] ***Pölling, R.*** Eine praxisnahe, schädigungsorientierte Materialbeschreibung von Stahlbeton für Strukturanalysen, Dissertation, Ruhr-Universität Bochum, Germany (2000).

[21] ***Ramm, E.*** (ed.) *Buckling of shells*, Berlin: Springer-Verlag (1982).

[22] ***Simo, J.C., Hughes, T.J.R.*** On the Variational Formulation of Assumed Strain Methods, J. Appl. Mech., 53, 51-54 (1986).

[23] ***Wolmir, A.S.*** *Biegsame Platten und Schalen.* Berlin: VEB Verlag für Bauwesen (1962).

[24] ***Zahlten, W.*** A contribution to the physically and geometrically nonlinear computer analysis of general reinforced concrete shells. Technical Report 90-2, Ruhr-Universität Bochum, Germany (1990).